INTER-CALIBRATION OF BRIGHTNESS TEMPERATURE FROM HY-2 SCANNING MICROWAVE RADIOMETER OVER OCEAN

Mingkun Liu(1) , Lei Guan(1) and Wei Zhao(2)
(1)Department of Marine Technology, Ocean University of China, Qingdao, China
(2) National Satellite Ocean Application Service, State Oceanic Administration, Beijing, China

Introduction Haiyang-2 (HY-2) is the first marine dynamic environmental satellite of China, that was launched on 16 August 2011. The scanning microwave radiometer (RM) onboard HY-2 has low frequency channels with the capability of observing sea surface temperature (SST) from space. The evaluation results showed the accuracy of SST from HY-2 RM is relatively low. The large difference between ascending and descending comparisons and the fluctuated bias and standard deviation indicate HY-2 RM is not well -calibrated. In this study, the Level 1B (L1B) brightness temperature of HY-2 RM are compared with the Global Precipitation Measurement (GPM) microwave radiometer (GMI) brightness temperature for the period from March 2014 to June 2016. The localized regression is used to correct the brightness temperature from HY-2 RM.

Comparison of HY-2 RM brightness temperature with GMI brightness temperature The HY-2 RM L1B brightness temperature products have been developed and distributed by the National Satellite Ocean Application Service (NSOAS) of the State Oceanic Administration (SOA). The GPM GMI L1B brightness temperature data is provided by the Japan Aerospace Exploration Agency (JAXA). The collocations of HY-2 RM and GPM GMI brightness temperature data are generated with the spatial window of 1° and the temporal window of 0.5 hour. The upper panel of Fig. 1 shows the three-year statistic of brightness temperature difference between HY-2 RM and GMI and the nether panel shows the variation of brightness temperature difference (RM minus GMI) against latitude. The comparison results show that the biases of brightness temperature difference from all channels are relatively large and the standard deviations of brightness temperature difference from 18GHz H-pol, 18GHz V-pol, 23GHz V-pol, and 37GHz H-pol channels are larger than 1K. Besides, the brightness temperature difference varies obviously with latitudes, especially for 18GHz H-pol, 18GHz V-pol and 37GHz H-pol channels. Except for the tiny difference of center frequencies and Earth incidence angle between RM and GMI, the large brightness temperature difference indicate some problems exit in the calibration of HY-2 RM, such as the Earth radiation intrusion into cold mirror.

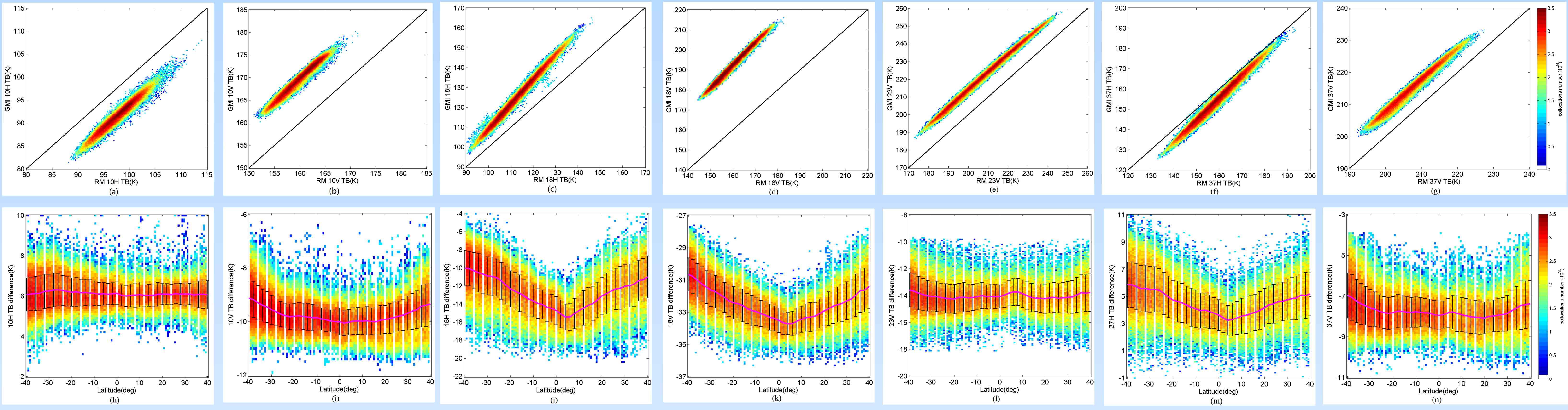

Fig. 1 Three-year statistic of brightness temperature difference between HY-2 RM and GMI [Fig. 1(a)] 10GHz H-pol, [Fig. 1(b)] 10GHz V-pol, [Fig. 1(c)] 18GHz H-pol, [Fig. 1(d)] 18GHz V-pol, [Fig. 1(e)] 23GHz V-pol, [Fig. 1(f)] 37GHz H-pol, [Fig. 1(g)], 37GHz V-pol] and the variation of brightness temperature difference (RM minus GMI) against latitude [Fig. 1(h)] 10GHz H-pol, [Fig. 1(i)] 10GHz V-pol, Fig. 1(j)] 18GHz H-pol, [Fig. 1(k)] 18GHz V-pol, [Fig. 1(l)] 23GHz V-pol, [Fig. 1(m)] 37GHz H-pol, [Fig. 1(n)], 37GHz V-pol]

Inter-calibration methology and the results Considering the dependence of brightness temperarture difference on latitudes, we use the different linear regression coefficients to correct the RM brightness temperature. The localized regression is trained to perform well over a relatively narrow range of latitudes and longitutes. Localized regressions are derived for 20 latitude reference values ranging from 40°S to 40°N and 36 longitude reference values ranging from 180°W to 180°E. Each regression is trained to perform well over a latitude/longitude of ±6° and ±10° centered on the reference latitude and longitude value. The matchup dataset between RM and GMI brightness temperature from March 2014 to Feburary 2015 is trained to obtain the localized coefficients. The matchup dataset from March 2015 to June 2016 is used to validate the inter-calibration algorithm. The corrected RM brightness temperature is retrived from a bi-linear interpolation of localized algorithms. The upper panel of Fig. 2 shows the statistic of brightness temperature difference between HY-2 RM and GMI after correction [Fig. 2(a)] 10GHz H-pol, [Fig. 2(b)] 10GHz V-pol, [Fig. 2(c)] 18GHz H-pol, [Fig. 2(d)] 18GHz V-pol, [Fig. 2(e)] 23GHz V-pol, [Fig. 2(f)] 37GHz H-pol, [Fig. 2(g)], 37GHz V-pol] and the nether panel shows the variation of brightness temperature difference (RM minus GMI) after correction against latitude. Table I shows the statistics of brightness temperature difference before and after correction between RM and GMI from March 2015 to June 2016. The large biases of original brightness temperature from all channels are removed. The standard deviations from 18GHz H-pol, 18GHz V-pol, and 37GHz H-pol channels are reduced significantly.

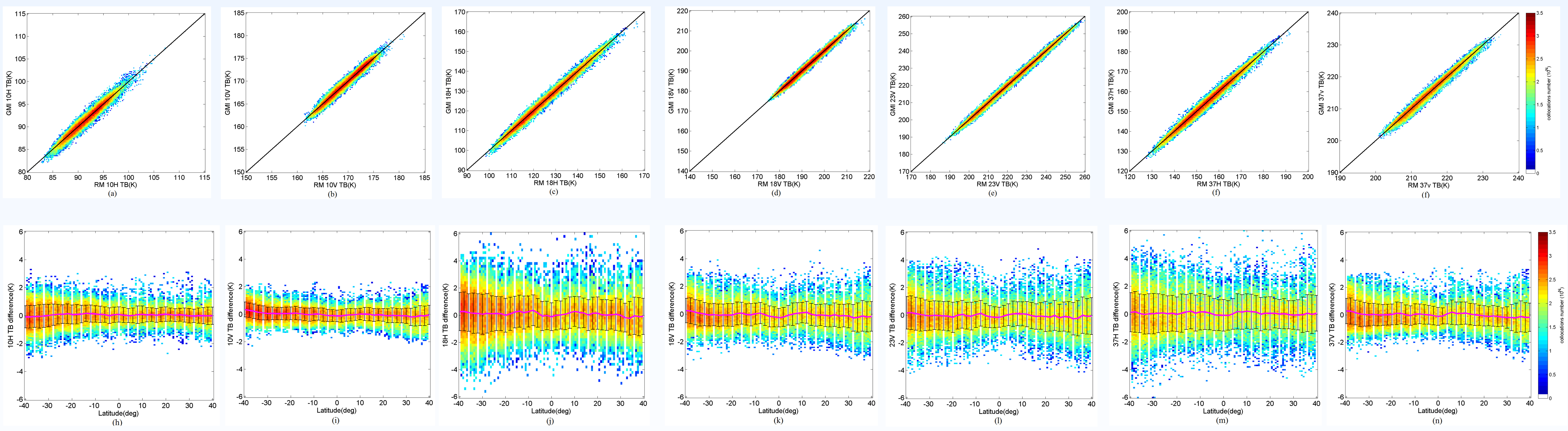

Fig. 2 Three-year statistic of brightness temperature difference between HY-2 RM and GMI after correction [Fig. 2(a)] 10GHz H-pol, [Fig. 2(b)] 10GHz V-pol, [Fig. 2(c)] 18GHz H-pol, [Fig. 2(d)] 18GHz V-pol, [Fig. 2e)] 23GHz V-pol, [Fig. 2(f)] 37GHz H-pol, [Fig. 2(g)], 37GHz V-pol] and the variation of brightness temperature difference (RM minus GMI) after correction against latitude [Fig. 2(h)] 10GHz H-pol, [Fig. 2(i)] 10GHz V-pol, Fig. 2(j)] 18GHz H-pol, [Fig. 2(k)] 18GHz V-pol, [Fig. 2(l)] 23GHz V-pol, [Fig. 2(m)] 37GHz H-pol, [Fig. 2 (n)], 37GHz V-pol]

Table I The statistics of original brightness temperature difference and corrected brightness temperature difference between RM and GMI from March 2015 to June 2016

	10GHz H-pol (before/after correction)	10GHz V-pol (before/after correction)	18GHz H-pol (before/after correction)	18GHz V-pol (before/after correction)	23GHz V-pol (before/after correction)	37GHz H-pol (before/after correction)	37GHz V-pol (before/after correction)
Bias (K)	6.14 / 0.03	-9.68 / 0.01	-12.33 / 0.10	-32.31 / -0.04	-14.03 / -0.04	4.74 / 0.05	-7.67 / 0.01
Standard Deviation (K)	0.64 / 0.63	0.57 / 0.50	2.62 / 1.22	1.34 / 0.83	1.07 / 1.01	1.66 / 1.24	0.87 / 0.81

Acknowledgements The research is supported by NSFC Project 41376105, NSFC-Shandong Joint Fund for Marine Science Research Centers (Grant No. U1406404), and SRFDP project 20130132110013.